Menoufia J. of Electronic Engineering Research (MJEER), Vol. 30, No. 2, Jul. 2021

Hybrid Precoding for Millimeter Wave Systems under Phase Noise Problem

1st *Muhammad R. El-Badry*
Electronic and communication dep.
Higher Institute of Engineering and Technology in El-Arish
North Sinai, Egypt
muhammadelbadry91@gmail.com

2nd *Taha E. Taha*
Electronic and communication dep.
Faculty of Electronic Engineering, Menoufia University
Mnoof, Egypt
taha117@hotmail.com

3rd *Mohamed G. El-Mashed*
Electronic and communication dep.
Faculty of Electronic Engineering, Menoufia University
Mnoof, Egypt
mohamed_elmashed@ymail.com

***Abstract*—Millimeter wave - mm Wave - communications has been considered as a key authorised technology for the fifth generation networks. Hybrid precoding, which refer to a blend of analog and digital precoding, can achieve high spectral and energy efficiencies. However a cost-effective alternative and power consumption are needed. So hybrid precoding strategies become promising solutions. In the higher carrier frequencies, especially the millimeter-wave range, there are significant degradations in the transmitted and received signals due to radio-frequency impairments such as phase noise introduced by the local oscillators (LO), which is the irregular difference among the phase of the local oscillator and the phase of the carrier signal. It's becoming a limiting factor in high data rate digital communication systems. In this research, we study the impact of phase noise on the performance of hybrid precoding structure in millimeter wave Multiple-Input Multiple-Output (MIMO) (mmWave MIMO) systems. Manifold optimization based alternating minimization algorithm is proposed. An optimization problem is formulated for phase noise issue in millimeter wave MIMO system. Results show that the impact of phase noise can degrade the system performance at higher RF chains.**

Keywords*— *Millimeter wave, hybrid precoding, alternating minimization, phase noise, optimization, fully-connected

I. INTRODUCATION

5G is the next generation of wireless networks. It has faster-lower latency and more flexibility, especially, after observing the amount of wireless voice and data communications which increasing at an exponential pace. Lately, mm Wave wireless systems are the best candidate technology for the next generation cellular communication [1]. To meet the volcanic demands of high-data-rate for the streaming media revolution and the capacity, there are many ways such as massive MIMO in the physical layer, network densification by diffusing small cells [2], and device to device -D2D- communication system [3]. Millimeter wave with frequencies between 30 and 300 GHz considered as the major candidate for overcome the imperfection of wireless frequency spectrum needed to cover a growing number of consumer devices. The characteristics of millimeter wave bands contain the availability of unexploited spectrum and control interference advantage as a result of the line-of-sight (LOS) property. Nevertheless, millimeter wave systems need a huge directional gain with respect to traditional systems to resist their huge path loss obstacle and losses due to oxygen and rain attenuation [4]. Large-sized phased-array antennas are introduced by millimeter wave system as a result of small wavelength which able to offer large beamforming gains to avoid path loss problem [3], [5], [6].

Precoding in simple words known as multiple data streams with beamforming, or we can say that precoding is the superposition of multiple beams for spatial multiplexing of several data streams. Beamforming and precoding are carried out digitally at baseband through digital precoders which can modify the phase and magnitude of the signals in traditional multi-antenna systems. Due to the huge price and power exhaustion of RF chains in mmWave systems (the huge price of mixed signal Components), and unluckily, the performance of analog strategies are suboptimal because of the limitations of analog beamforming hardware such as the difficulty of controlling signal amplitude and the potentially low-resolution signal phase control [7]. Wherefore, a structure of hybrid precoding has recently more attractive with a small number of RF chains, thanks to its ability to obtain high data rates with low energy consumption hardware.

RF chain is a cascade of electronic components, which including analog-to-digital converters (ADCs) and frequency mixer. It is nonlinear electrical circuit that designed to sum and difference frequency at a single output port from two signals applied to its input. One of this two input ports is usually the local oscillator (LO) device, it is one of the main components of radio frequency system, which in charge of the (up/down) conversion of a particular channel. In detail, it has the most important role on modulation and demodulation processes [8].

With reference to the mapping from RF chains to antennas, the hybrid precoding transceiver architectures can be categorized into the partially and fully connected structures. Talking about the constraints of transmitted signal, in fact there are many of factors that corrupt this transmitted signal such as phase noise and amplitude noise of the local oscillator, thermal noise, nonlinear behavior of active components and multipath effects.

In this article, we will discuss the effect of phase noise problem on hybrid precoding algorithms based on the principle of alternating minimization (AltMin), which near to the performance of the optimal fully digital precoder. As mentioned in [5], decreasing the Euclidean distance between hybrid precoder and the fully digital precoder can apparently achieve maximum the spectral efficiency of mmWave system, which makes a hybrid precoder design as a problem with respect to unit modulus constraints. However, there are no studies that cover the issue of hybrid precoding in millimeter wave systems under phase noise problem.

The main concern of the paper is to study the effect of phase noise issue on the hybrid design precoder in millimetre wave MIMO systems, which can create performance degradation for the whole system [9]. By adopting alternating minimization and phase extraction alternating minimization algorithms as the main design rule, the precoder design problem is divided into sub-problems by optimizing the analog precoder and the digital precoder with respect to phase noise problem.

The rest of the paper is tidied as followings. In Section II, the system model under phase noise model is introduced. Also, the problem formulation related to phase noise with phase locked loop is provided. In Section III, the precoding techniques for the proposed system with fully-connected structure are explained. The results are clarify at Section IV. Finally, the conclusion is provided in Section V.

II. System Model Under Phase Noise Problem

A. System Model

A single-user mmWave MIMO system is shown in Fig. 1. The information signal, $\boldsymbol{x}$is affected by the fading channel, $\boldsymbol{h}$. The receiver noise is assumed to beadditive noise $\boldsymbol{v}$. The data streams, N_s are sent from transmit antennas, N_t and collected by receive antennas, N_r. We consider the numbers of RF chains at the transmitter and receiver are stand for N_{RF}^t and N_{RF}^r, respectively, and subject to constraints $N_s \leq N_{RF}^t \leq N_t$ and $N_s \leq N_{RF}^r \leq N_r$. As known oscillators used in this system suffer from phase instabilities, which are referred to as oscillator phase noise. It's can limit the performance of high speed communication systems since it results in time varying channels and rotation of the signal constellation from symbol to another. The transmitted signal can be expressed as:

$$\mathbf{X}_l = \mathbf{s}\,\mathbf{F}_{RF}\mathbf{F}_{BB} \qquad (1)$$

where $\mathbf{s}$ is the $N_s \times 1$symbol vector such that, $\mathbb{E}[\boldsymbol{ss}^H] = \mathbf{I}_{N_s}/N_s$. The receiving signal in cell i at a given channel use $t \in \{1, \ldots, T\}$ of a physical RF transceivers system model experiencing phase noise drawback is mathematically delineated as the following:

$$\mathbf{y}_i(t) = \mathbf{D}_{\varphi_i(t)} \sum_{l=1}^{L} \mathbf{H}_{il}\mathbf{X}_l(t) + \boldsymbol{v}_i(t) \qquad (2)$$

where $\mathbf{D}_{\varphi_i(t)}$ is the phase noise, which describes the multiplicative phase drifts and is as follows:

$$\boldsymbol{D}_{\varphi_i(t)} \triangleq \mathrm{diag}\left(e^{jd_1(t)}, \cdots, e^{jd_n(t)}\right) \qquad (3)$$

where j is the imaginary unit and the variable $d_n(t)$ is the phase-drift at the nth receive antenna at time t. Motivated by the standard, $d_n(t)$ follows a Wiener process $d_n(t) \sim N(d_n(t-1), \delta)$, which equals the previous realization $d_n(t-1)$ plus an independent Gaussian innovation of variance δ. The phase drifts can be either correlated or independent between the antennas. For the case of co-located arrays with a common local oscillator for all antennas, the phase-drifts $d_n(t)$ are identical for all$n = 1, \ldots, N$.

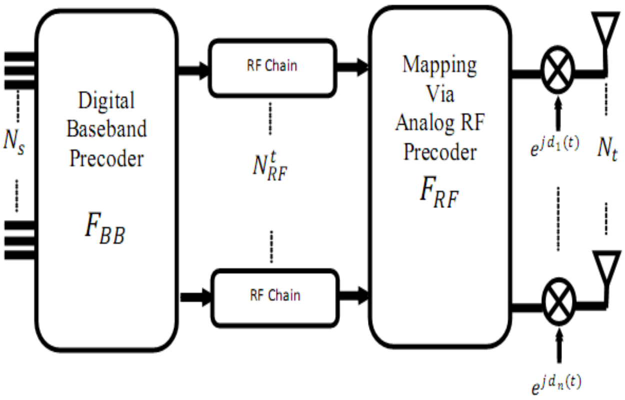

(a) mmWave MIMO transmitter architecture.

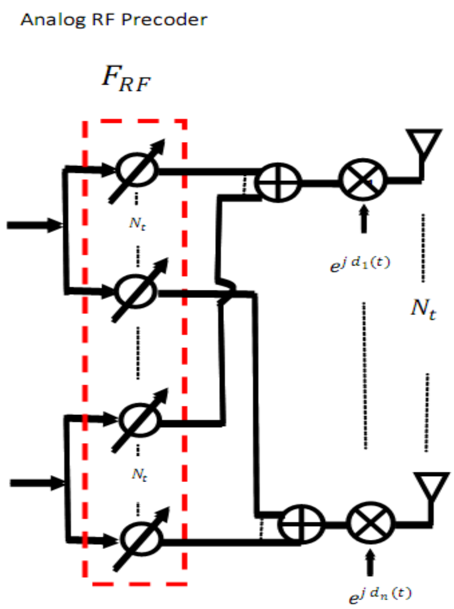

(b) The mapping strategy for the fully-connected structure.

Fig. 1: The proposed structure of hybrid precoding in mmWave MIMO systems under phase noise.

As shown in Fig. 1(a), in the data stream side, the hybrid precoder consists of an $N_{RF}^t \times N_s$ digital baseband precoder, $\mathbf{F}_{BB}$. In transmitted antenna side, the hybrid precoder consists of an $N_t \times N_{RF}^t$ analog RF precoder, F_{RF}. The constraint of the normalized power transmitted is given by

$\|\delta^2 \mathbf{F}_{RF}\mathbf{F}_{BB}\|_F^2 = N_S$. For simplification, we tend to think about a narrowband block fading propagation channel [2], whereas the extension to broadband OFDM systems. Thus, the received signal after the decoding process is given as:

$$\mathbf{y}_i(t) = \sqrt{\rho}\mathbf{D}_{\varphi_i(t)}\mathbf{W}_{BB}^H\mathbf{W}_{RF}^H\mathbf{H}\mathbf{F}_{RF}\mathbf{F}_{BB}\mathbf{s} + \mathbf{W}_{BB}^H\mathbf{W}_{RF}^H\boldsymbol{n} \quad (4)$$

where $\boldsymbol{D}_{\varphi_i(t)}$ is the pahse noise, ρ refer to the average received power, $\mathbf{W}_{BB}$ is the digital baseband decoder at the receiver part, $\mathbf{W}_{RF}$ is the analog RF decoder at the receiver side, $\mathbf{H}$ is the channel matrix, and $\boldsymbol{n}$stands for the noise vector of independent and identically distributed $\mathcal{CN}(0, \sigma_{\alpha,i}^2)$. As known in [10], we can achieve the channel state information (CSI) by channel estimation process at the receiver side, then send the feedback to the transmitter side. We tend to assume the perfect case of CSI which make it known at the both transmitter and receiver parts. When the transmitted symbols follow a normal distribution, the equation that describes the spectral efficiency that we can obtained is as follows:

$$\boldsymbol{R} = \log\det\left(\mathbf{I}_{Ns} + \frac{\rho\delta^2}{\sigma_{nN_S}^2}(\mathbf{W}_{RF}\mathbf{W}_{BB})^\dagger\mathbf{H}\mathbf{F}_{RF}\mathbf{F}_{BB} \times \boldsymbol{F}_{BB}^H\boldsymbol{F}_{RF}^H\mathbf{H}^H\mathbf{W}_{RF}\mathbf{W}_{BB}\right) \quad (5)$$

where δ^2 is the variance of phase noise, $\mathbb{E}\left[\boldsymbol{D}_{\phi_i(t)}\boldsymbol{D}_{\phi_i(t)}^\dagger\right] = \delta^2$, take in consideration that the analog precoders ($\mathbf{F}_{RF}$, $\mathbf{W}_{RF}$) are implemented with phase shifters, which modify the signal's phase. So the nonzero entries of $\mathbf{F}_{RF}$ and $\mathbf{W}_{RF}$ must satisfy the unit modulus constraints for nonzero elements, $|(\mathbf{F}_{RF})_{i.j}| = |(\mathbf{W}_{RF})_{i.j}| = 1$. As demonstrated in Fig. 1(b), the mapping strategy for the fully connected hybrid structure, the signal output of each RF chain is delivered to all antennas, so this structure has the benefit of full beamforming gain for each RF chain.

B. Channel Model

By consideration of aSaleh-Valenzuela clustered channel model for mmWave propagation environment in order to high path loss in free space [11]. It describes the mmWave channel matrix $\mathbf{H}$ as follows:

$$\mathbf{H} = \sqrt{\frac{N_t\ N_r}{N_{cl}\ N_{ray}}}\sum_{i=1}^{N_{cl}}\sum_{l=1}^{N_{ray}} \alpha_{il}\boldsymbol{a}_r(\phi_{il}^r, \theta_{il}^r)\,\boldsymbol{a}_t(\phi_{il}^t, \theta_{il}^t)^H \quad (6)$$

where N_{ray} and N_{cl} represent the number of rays and the number of clusters in each cluster, respectively and α_{il}refers to the gain of the lth ray in the ith propagation cluster. Assuming that $\alpha_{il}$is i.i.d , which follows the distribution $\mathcal{CN}(0, \sigma_{\alpha,i}^2)$ and $\sum_{i=1}^{N_{cl}}\sigma_{\alpha,i}^2 = \hat{\gamma}$, which is the normalization factor to satisfy $\mathbb{E}[\|\boldsymbol{H}\|_F^2] = N_t N_r$. As well, $\boldsymbol{a}_r(\phi_{il}^r, \theta_{il}^r)$and $\boldsymbol{a}_t(\phi_{il}^t, \theta_{il}^t)^H$represent the receive and transmit array response vectors, whereϕ_{il}^r,ϕ_{il}^t and θ_{il}^r, $\theta_{il}^t$are refer to azimuth angle and elevation angle of arrival and departure, respectively.

Suppose that $\sqrt{N}\times\sqrt{N}$ antenna elements of uniform square planar array. Thus, we can write the array response vector identical to the lth ray in the ith cluster as the follows:

a

= (7)

where r is the antenna spacing and λ is the wavelength of the signal. The bounds of antenna indices p and q are $0 \le p < \sqrt{N}$ and $0 \le q < \sqrt{N}$, respectively in the 2D-plane.

C. Problem Formulation

The corresponding problem formulation for the precoders design under phase noise is shown as the follows:

$$\underset{\mathbf{F}_{RF},\mathbf{F}_{BB}}{\text{minimize}} \qquad \left\|\mathbf{F}_{opt} - \delta^2\mathbf{F}_{RF}\mathbf{F}_{BB}\right\|_F \quad (8)$$

where $\boldsymbol{F}_{opt}$ refers to the optimum fully digital precoder, δ^2 is the variance of phase noise. We assume that the range of $\delta$is between 10^{-4} and 10^{-1}. $\mathbf{F}_{RF}$ and $\mathbf{F}_{BB}$ are the optimized analog and digital precoders. In addition to the feasible set $\mathcal{A}_f$ of the analog precoder the constraints of the unit modulus for the fully connected structure, and it is different for several hybrid precoding structures. As mentioned at [5], there is a relation between this minimization and the spectral efficiency, which indicate that the spectral efficiency will increase as a result of this minimization. Let us first show that our problem can be considered as a matrix factorization problem, by using Alt-Min tool, and then we show the effect of phase noise on the system performance.

III. PRECODING TECHNIQUES

In this section, we illustrate different design for precoding techniques to solve the optimization problem in (8).

A. Digital Baseband Precoder Design

By fixing analog precoder $\mathbf{F}_{RF}$, then we consider to design the digital precoder $\mathbf{F}_{BB}$. Thus, the problem in (8) can be restated as:

(9)

which has a well-known least squares solution given by:

(10)

B. Identify Analog RF Precoder Design via Manifold Optimization

The feasible set, $\mathcal{A}_f$ of the analog precoder can be specified by $\left|(\mathbf{F}_{RF})_{i,j}\right| = 1$, as eachRF chain is connected to all the antennas. In the next alternating step, we fix $\mathbf{F}_{BB}$ and seek an analog precoder which optimizes the problem as:

$$\underset{\mathbf{F}_{RF}}{\text{minimize}} \qquad \left\|\mathbf{F}_{opt} - \delta^2 \mathbf{F}_{RF}\mathbf{F}_{BB}\right\|_F^2 \tag{11}$$

The unit modulus constraints are intrinsically non-convex, so it is not easy to find optimal solution. In this paper, we propose a manifold optimization algorithm to find a solution of problem (11). Let us first define the terminologies in manifold optimization. Fig. 2 shows a manifold, $\mathcal{M}$, which is a topological space that make a Euclidean space near each point [12]. Each point on a manifold has a homeomorphic neighborhood to the Euclidean space. The space, $\mathrm{T}_x\mathcal{M}$ at a point x on the manifold $\mathcal{M}$ is contain tangent vectors, ξ_x of the curves and γthrough the point x. A common Riemannian manifold is equipped with an inner product defined on the tangent spaces $\mathrm{T}_x\mathcal{M}$, called the Riemannian metric, which facilities the calculation distances and angles on manifolds.

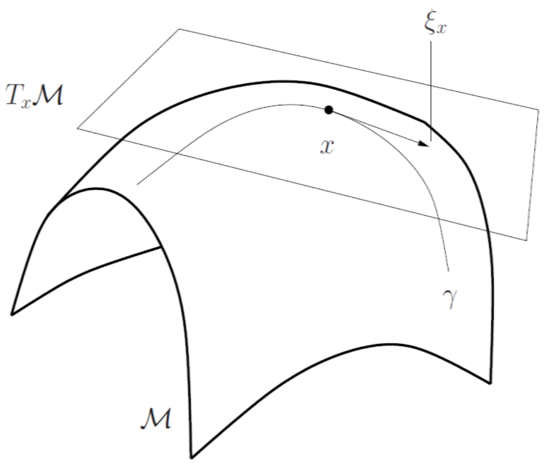

Fig. 2: The tangent space and tangent vector of a Riemannian manifold [16].

An optimization over a Riemannian manifold is locally analogous than a Euclidean space with smooth constraints. Therefore, a conjugate gradient algorithm in Euclidean spaces can find its counterpart on the specified Riemannian manifolds. Firstly, we illustrate this counterpart. Let the complex plane $\mathbb{C}$ with the Euclidean metric can be expressed as:

(12)

which is equivalent to treating $\mathbb{C}$ as $\mathbb{R}^2$with the canonical inner product. Let the complex circle as:

$$\mathcal{M}_{\mathrm{cc}} = \{x \in \mathbb{C}: x^* x\} = 1 \tag{13}$$

The directions of point x on the manifold $\mathcal{M}_{\mathrm{cc}}$along which it can move are characterized by the tangent vectors ξ_x. Then the tangent space at the point $x \in \mathcal{M}_{\mathrm{cc}}$ is:

$$\mathrm{T}_x\mathcal{M}_{\mathrm{cc}} = \{\mathrm{z} \in \mathbb{C}: z^* x + x^* \mathrm{z} = 2\langle x, z\rangle = 0\} \tag{14}$$

Note that the vector $x = \mathrm{vec}(\mathbf{F}_{RF})$ forms a complex circle manifold

$$\mathcal{M}_{cc}^m = \{\mathbf{x} \in \mathbb{C}^m : |\mathbf{x}_1| = |\mathbf{x}_2| = \cdots = |\mathbf{x}_m| = 1\} \tag{15}$$

where $m = N_t N_{RF}^t$. Therefore, the search space of the optimization problem (11) is over a product of m circles in the complex plane, which is a Riemannian submanifold of $\mathbb{C}^m$ with the product geometry. Hence, the tangent space at a given point $\mathbf{x} \in \mathcal{M}_{cc}^m$ is:

$$\mathrm{T}_x\mathcal{M}_{cc}^m = \left\{\mathbf{z} \in \mathbb{C}^m : \Re\{\mathbf{z} \circ \mathbf{x}^*\} = 0_m\right\}. \tag{16}$$

One of the tangent vectors represents the direction of the greatest decrease of a function. The gradient at $\mathbf{x}$ is a tangent vector, $\mathrm{grad}f(\mathbf{x})$ given by the orthogonal projection of the Euclidean gradient, $\nabla f(\mathbf{x})$ onto the tangent space, $\mathrm{T}_x\mathcal{M}_{cc}^m$ [12]:

$$\mathrm{grad}f(\mathbf{x}) = \mathrm{Proj}_{\mathbf{x}}\nabla f(\mathbf{x}) \tag{17}$$

where the Euclidean gradient of the cost function in (11) is:

$$\nabla f(\mathbf{x}) = -2\left(\mathbf{F}_{BB}^* \otimes \mathbf{I}_{N_t}\right)\left[\mathrm{vec}(\mathbf{F}_{opt}) - (\mathbf{F}_{BB}^{\mathrm{T}} \otimes \mathbf{I}_{N_t})\mathbf{x}\right]. \tag{18}$$

Solving this Euclidean gradient involves some techniques on complex-valued matrix derivatives, the details can be found in [13]. Retraction process is used to map a vector from the tangent space onto the manifold area. It determines the destination on the manifold when moving along a tangent vector. The retraction of a tangent vector $\alpha\mathbf{d}$ at point $\mathbf{x} \in \mathcal{M}_{cc}^m$ is:

$$\begin{gathered}\mathrm{Retr}_{\mathbf{x}}: \mathrm{T}_{\mathrm{x}}\mathcal{M}_{cc}^m \to \mathcal{M}_{cc}^m : \\ \alpha\mathbf{d} \longmapsto \mathrm{Retr}_{\mathrm{x}}(\alpha\mathbf{d}) = \mathrm{vec}\left[\frac{(\mathbf{x} + \alpha\mathbf{d})_i}{|(\mathbf{x} + \alpha\mathbf{d})_i|}\right]\end{gathered} \tag{19}$$

With the tangent space, Riemannian gradient and retraction process, a line search based conjugate gradient method, can be applied to solve the analog precoder in (11) as showed in Algorithm 1. It applies the Armijo backtracking line search step and Polak-Ribiere parameter. Steps 7 and 8 involve the processes between different tangent spaces $\mathrm{T}_{\mathbf{x}_k}\mathcal{M}_{cc}^m$ and $\mathrm{T}_{\mathbf{x}_{k+1}}\mathcal{M}_{cc}^m$. A mapping between two tangent vectors $\mathbf{d}$ from $\mathbf{x}_k$ to $\mathbf{x}_{k+1}$ is:

$$\mathrm{Transp}_{\mathbf{x}_k \to \mathbf{x}_{k+1}}: \mathrm{T}_{\mathbf{x}_k}\mathcal{M}_{cc}^m \to \mathrm{T}_{\mathbf{x}_{k+1}}\mathcal{M}_{cc}^m : \tag{20}$$

$$\mathbf{d} \mapsto \mathbf{d} - \Re\{\, \mathbf{d} \circ \mathbf{x}_{k+1}^{*}\} \circ \mathbf{x}_{k+1}$$

Algorithm 1: Analog Precoding Based on Manifold Optimization
Input: F_{opt}, F_{BB}, $\mathbf{x}_0 \in \mathcal{M}_{cc}^{m}$ 1: $\mathbf{d}_0 = -\mathrm{grad}\, f(\mathbf{x}_0)$ and $k = 0$; 2: **repeat** 3: Choose Armijo backtracking line search step size α_k; 4: Find the next point $\mathbf{x}_{k+1}$ using retraction process in (19): $\mathbf{x}_{k+1} = \mathrm{Retr}_{\mathbf{x}_k}(\alpha_k \mathbf{d}_\mathrm{k})$; 5: Determine Riemannian gradient $\mathbf{g}_{k+1} = \mathrm{grad}\, f(\mathbf{x}_{k+1})$ according to (17) and (18); 6: Calculate the vector transports $\mathbf{g}_k^{+}$ and $\mathbf{d}_k^{+}$of gradient $\mathbf{g}_k$ and conjugate direction $\mathbf{d}_\mathrm{k}$ from $\mathbf{x}_k$ to $\mathbf{x}_{k+1}$ 7: Choose Polak-Ribiere parameter β_{k+1}; 8: Compute conjugate direction $\mathbf{d}_{k+1} = -\mathbf{g}_{k+1} + \beta_{k+1}\mathbf{d}_k^{+}$; 9: $k \leftarrow k$ +1; 10: Until a stopping criterion triggers.

C. Hybrid Precoder Design

The hybrid precoder design via alternating minimization in the MO-AltMin Algorithm by solving problems (9) and (11) iteratively. To satisfy the power constraint in (8), we normalize $\mathbf{F}_{BB}$ by a factor of $\frac{\sqrt{N_s}}{\|\delta^2 \mathbf{F}_{RF}\mathbf{F}_{BB}\|_\mathrm{F}}$ at Step 7.

MO-AltMin Algorithm: Hybrid Precoding
Input: $\mathbf{F}_{opt}$, δ 1: Construct $\mathbf{F}_{RF}^{(0)}$ with random phases and set k = 0; 2: **repeat** 3: Fix $\mathbf{F}_{RF}^{(\mathrm{k})}$ and $\mathbf{F}_{BB}^{(\mathrm{k})} = {\delta^2}^{\dagger}\mathbf{F}_{RF}^{(\mathrm{k})\dagger}\mathbf{F}_{opt}$; 4: Optimize $\mathbf{F}_{RF}^{(\mathrm{k}+1)}$ using Algorithm 1 when $\mathbf{F}_{BB}^{(\mathrm{k})}$is fixed; 5: $k \leftarrow k$ +1; 6: **Until** a stopping criterion triggers; 7: For the digital precoder at the transmit end, normalize $\widehat{\mathbf{F}}_{BB} = \frac{\sqrt{N_s}}{\|\delta^2 \mathbf{F}_{RF}\mathbf{F}_{BB}\|_\mathrm{F}}\mathbf{F}_{BB}$.

IV. RESULTS

The performance of the proposed mm-Wave MIMO systems under phase noise and different hybrid precoding techniques is evaluated. The number of antennas at BS and user are 144 and 16 antennas, respectively. We assume uniform planar arrays at all the transceivers. To reduce the cost and power consumption, we consider the numbers of RF chains at the transmitter and receiver are $N_{RF}^{t} = KN_s$ and $N_{RF}^{r} = N_s$, respectively.

Firstly, we illustrate the spectral efficiency achieved by different precoding techniques when the number of RF chains is equal to that of the data streams, i.e., $N_{RF}^{t} = N_{RF}^{r} = N_s = 4$ as shown in Fig. 3 and Fig. 4. With phase noise $\delta = 10^{-4}$, the proposed system with analog precoder achieves significantly lower spectral efficiency than the digital and hybrid precoders as in Fig. 3. The hybrid precoder can achieve near- performance to the digital one. When we increase impact of phase noise as in Fig. 4, the system spectral efficiency is reduced. So, the phase noise has a little impact on the proposed system when the number of RF chains is small.

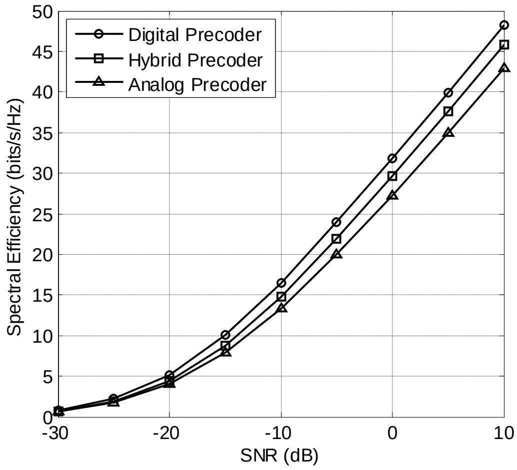

Fig. 3: Spectral efficiency versus SNR for the proposed mm-Wave MIMO systems under phase noise when $N_{RF}^{t} = N_{RF}^{r} = N_s = 4$ and $\delta = 10^{-4}\mathrm{rad}^2$.

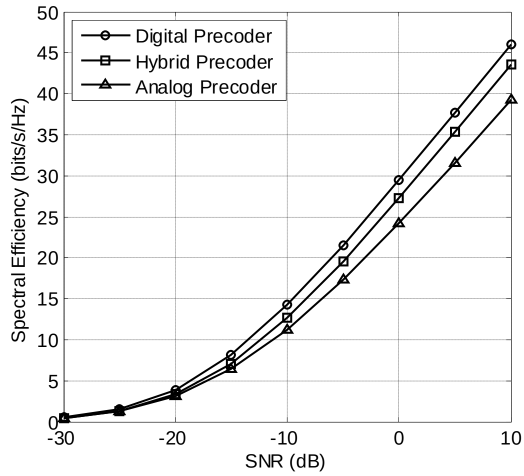

Fig. 4: Spectral efficiency versus SNR for the proposed mm-Wave MIMO systems under phase noise when $N_{RF}^{t} = N_{RF}^{r} = N_s = 4$ and $\delta = 10^{-2}\mathrm{rad}^2$.

Secondly, we increase the number of RF chains to $N_{RF}^{t} = N_{RF}^{r} = N_s = 8$ as in Fig. 5 and Fig. 6 at phase noise $\delta = 10^{-4}$. The spectral efficiency is improved with the three precoding techniques. The system performance with hybrid precoder is close to digital precoder. With increasing the impact of phase noise as in Fig. 6, the proposed system with analog precoder is more affected by phase noise. Also, there is a gap between digital and hybrid precoder. Finally, we can conclude that the impact of phase noise can degrade the system performance at higher RF chains.

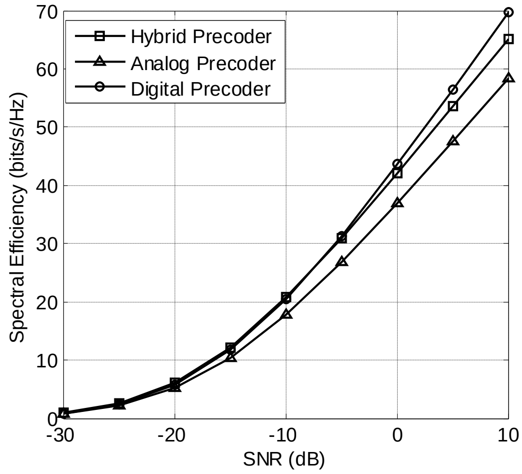

Fig. 5: Spectral efficiency versus SNR for the proposed mm-Wave MIMO systems under phase noise when $N_{RF}^{t} = N_{RF}^{r} = N_s = 8$ and $\delta = 10^{-4}\mathrm{rad}^2$.

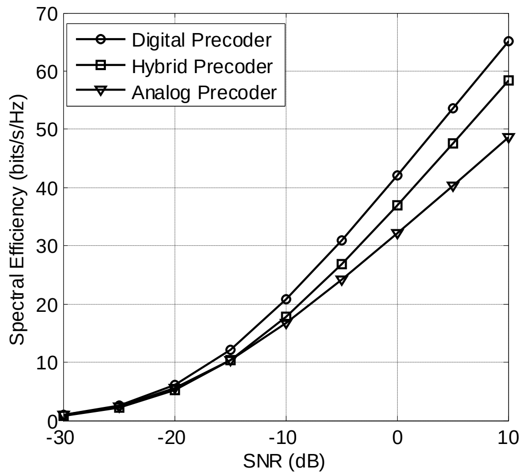

Fig. 6: Spectral efficiency versus SNR for the proposed mm-Wave MIMO systems under phase noise when $N_{RF}^{t} = N_{RF}^{r} = N_s = 8$ and $\delta = 10^{-2}\mathrm{rad}^2$.

V. CONCLUSION

In this paper, the impact of phase noise on the performance of hybrid precoding structure in Millimeter wave MIMO systems has been investigated. Manifold optimization based alternating minimization algorithm has been proposed. An optimization problem has been formulated to study spectral efficiency. Results show that the impact of phase noise can degrade the system performance at higher RF chains.

REFERENCES

[1] J. H. Lee and Y. H. Lee, "AF relaying for millimeter wave communication systems with hybrid RF/baseband MIMO processing," in *IEEE International Conference on Communications (ICC)*, pp. 5838–5842, 2014.

[2] X. Yu, J.-C. Shen, J. Zhang, and K. B. Letaief, "Alternating Minimization Algorithms for Hybrid Precoding in Millimeter Wave MIMO Systems," IEEE Journal of Selected Topics in Signal Processing, vol. 10, no. 3, pp. 485–500, 2016.

[3] K. Doppler, M. Rinne, C. Wijting, C. Ribeiro, and K. Hugl, "Device-to-device communication as an underlay to LTE-advanced networks," *IEEE Communications Magazine*, vol. 47, no. 12, pp. 42–49, 2009.

[4] S. Hur, T. Kim, D. J. Love, J. V. Krogmeier, T. A. Thomas, and A. Ghosh, "Millimeter Wave Beamforming for Wireless Backhaul and Access in Small Cell Networks," *IEEE Transactions on Communications*, vol. 61, no. 10, pp. 4391–4403, 2013.

[5] O. E. Ayach, S. Rajagopal, S. Abu-Surra, Z. Pi, and R. W. Heath, "Spatially Sparse Precoding in Millimeter Wave MIMO Systems," *IEEE Transactions on Wireless Communications*, vol. 13, no. 3, pp. 1499–1513, 2014.

[6] I. Khan, M. H. Alsharif, M. H. Zafar, M. O. Alassafi, M. Ashraf, Y. Huang, J. Kim, and J. H. Kim, "An Efficient Algorithm for mmWave MIMO Systems," Symmetry, vol. 11, no. 6, p. 786, 2019.

[7] A. Alkhateeb, O. E. Ayach, G. Leus, and R. W. Heath, "Hybrid precoding for millimeter wave cellular systems with partial channel knowledge," *2013 Information Theory and Applications Workshop (ITA)*, 2013.

[8] V. Fialho, F. Fortes, and M. Vieira, "Local Oscillator Phase Noise Influence on Single Carrier and OFDM Modulations*," IFIP Advances in Information and Communication Technology Technological Innovation for the Internet of Things*, pp. 513–520, 2013.

[9] X. Cheng and N. Lou, "Phase noise suppression in multi-gigabit millimeter wave systems," *2016 IEEE International Conference on Communication Systems (ICCS)*, 2016.

[10] A. Alkhateeb, O. E. Ayach, G. Leus, and R. W. Heath, "Channel Estimation and Hybrid Precoding for Millimeter Wave Cellular Systems," *IEEE Journal of Selected Topics in Signal Processing*, vol. 8, no. 5, pp. 831–846, 2014.

[11] T. S. Rappaport, R. W. Heath, R. C. Daniels, and J. N. Murdock, Millimeter wave wireless communications. Upper Saddle River: Pearson Education, 2015.

[12] P.-A. Absil, R. Mahony, and R. Sepulchre, Optimization algorithms on matrix manifolds. Princeton: Princeton Univ. Press, 2009.

[13] A. Hjørungnes, Complex-valued matrix derivatives: with applications in signal processing and communications. Cambridge: Cambridge University Press, 2011.